MINERALOGICAL MAGAZINE, DECEMBER 1980, VOL. 43, PP. 1015-23

The eosphorite-childrenite series associated with the Li-Mn-Fe phosphate minerals from the Buranga pegmatite, Rwanda

A.-M. FRANSOLET

Institut de Minéralogie, Université de Liège, Place du Vingt-Août, B-4000 Liège, Belgium

SUMMARY. From the Buranga pegmatite, Rwanda, three occurrences of eosphorite-childrenite series minerals are described in assemblages of Li-Fe-Mn-bearing phosphates and in relationship with quartz-feldspar masses in close association with these assemblages.

Electron-microprobe analyses of these terms (Mn,Fe) $AlPO_4(OH)_2 \cdot H_2O$ afford the following $Fe_t/(Fe_t + Mn)$ ratios: 0.548, 0.341, and 0.200. However, thanks to an investigation of the refractive indices and pleochroism, the presence of ferric iron is demonstrated and an oxidation phenomenon, similar to that previously known in rockbridgeite, is suggested to explain the existence of oxidized eosphorite. The oxychildrenite problem is raised again.

The $Fe_t/(Fe_t + Mn)$ ratios characterizing the eosphorite *sensu lato* would be correlated with the Fe and Mn content of the associated major phosphates, the chemical analyses of which are also provided. The investigation of the structural relationships shows that eosphorite might form a paragenesis with montebrasite and that these phosphates replace Na- or K-feldspars by a hydrothermal process. Owing to the apparent dependence of the chemical properties of the couple eosphorite-montebrasite on those of the earlier-formed phosphates, it seems likely that the formation period of eosphorite-childrenite series minerals was prior to the oxidation and ferrisicklerite-heterosite formation.

IN the Buranga pegmatite, Rwanda, Von Knorring (1965) has mentioned the presence of an eosphorite-childrenite series member associated with brasilianite and scorzalite. Detailed investigations of the Fe- and Mn-rich phosphate minerals assemblages from that locality have also revealed occurrences of terms of this isomorphic series in three different associations.

The eosphorite-childrenite series is frequently recorded, but quoted as an accessory product in the phosphate mineral associations from the granitic pegmatites; this research, based only on the Buranga mine example, tends to show that new indications about the geochemical features, especially about the behaviour of the Fe/Mn ratio during the oxidation processes, can be derived from an investigation of this series too. From one association to another the Fe/Mn ratio of (Mn,Fe) $AlPO_4(OH)_2 \cdot H_2O$ varies appreciably and a comparison is established with the same ratio characterizing the earlier-formed phosphates. The eosphorite-childrenite series members, sometimes associated with montebrasite, appear as hydrothermal products of Na- or K-feldspars altered by phosphorus-rich solutions.

Analytical methods

The role of the eosphorite-childrenite series in the evolution of the Fe- and Mn-rich phosphate minerals associations requires an petrologic investigation of their structural relationships, based on an accurate determination of the Fe/Mn ratio. These data were collected by the electron microprobe on X-rayed and optically investigated material from associations for which the evolution process has been previously described (Fransolet, 1975, 1976, and 1977).

The chemical analyses were performed by the fully automatic Camebax electron microprobe (BRGM-CNRS) following the analytical procedure of Remond *et al.* (1977). The operating conditions are: incident energy 15 keV, beam current 10 nA and counting time 5s. P, Al, Fe, Mn, Mg, and Ca were calibrated with Kabira graftonite (Von Knorring, 1970) and synthetic Al_2O_3 and MgO. Ten-point analyses were made on a well-developed eosphorite-childrenite section and three other analyses were repeated on a few adjoining sections. In this way small variations of the Fe/Mn ratio were detected, with no particular distribution into the associations. Only the average of these analyses (Table I) will be considered in the discussion. The Al_2O_3 contents are systematically a little lower than those in the literature, which could be attributed to the choice of the Al_2O_3 standard when a homogeneous aluminium phosphate is unavailable.

Any eosphorite-childrenite series member is easily identified by the X-ray diffraction but the Fe/Mn ratio cannot be specified. An Mn-rich member is characterized by a larger cell than a Fe-rich one (Strunz and Fisher, 1957); but there is a considerable difference between the cell dimensions of Newry eosphorite obtained by these authors and the results of Hanson (1966). Presently the data are lacking to correlate the Fe/Mn ratios and the cell dimension variations. Such correlations cannot be proposed for the Buranga material because the number of investigated specimens is too low and the small amount of available material from each association precludes a chemical determination of the cations especially ferrous iron. While ernstite $(Mn_{1-x}Fe^{3+}_x)AlPO_4(OH)_{2-x}O_x$, which is rather similar to eosphorite (Seeliger and Mücke, 1970), can be distinguished by X-ray diffraction, the powder patterns of oxychildrenite and childrenite are practically identical (Fleisher, 1965).

According to Hurlbut (1950) and Winchell (1958) the Fe/Mn ratios are optically determinable. The optical properties of the Buranga minerals were observed in the thin sections and the measurement of the refractive indices was carried out on isolated grains by immersion and wavelength variation methods. The relationships suggested by Hurlbut (1950) and Winchell (1958) have been tentatively used to check the Fe/(Fe + Mn) ratios. However, the minerals concerned here frequently display a pleochroism, very variable and sometimes intense, differently distributed into the monomineralic sections. These yellow or orange zones in connection with the cleavages and the fractures are particularly dispersive and the abnormal bronze or deep-blue colours screen the birefringence. In the eosphorite series the pleochroism has been scarcely mentioned for the minerals from North Groton and Red Hill, Maine (Hurlbut, 1950). This property, pretty constant in Buranga, gives rise to a determination problem (see below) and tends to restrict considerably the usefulness of the correlations between the refractive indices and the iron content, apparently established with colourless or weakly tinged specimens.

TABLE I. *Eosphorite-childrenite series, Buranga pegmatite. Chemical compositions*

	I	II	IIIa	IIIb
P_2O_5	30.97	30.69	30.74	30.45
Al_2O_3	21.77	21.50	21.82	21.62
FeO*	16.59	10.63	6.14	6.03
MnO	13.55	20.30	24.30	24.44
MgO	0.07	0.07	0.00	0.00
CaO	0.09	0.07	0.02	0.10
Cations calculated on the basis of 8 PO_4				
Al^{3+}	7.83	7.80	7.91	7.91
Fe^{2+}	4.24	2.74	1.58	1.56
Mn^{2+}	3.50	5.30	6.33	6.42
Mg^{2+}	0.03	0.03	—	—
Ca^{2+}	0.03	0.02	0.01	0.03
ΣR^{2+}	7.80	8.09	7.92	8.01
$Fe_t/(Fe_t+Mn)$	0.548	0.341	0.200	0.195

* Total iron as FeO.

Chemical analyses performed by the Camebax electron microprobe (BRGM-CNRS). Analyst: C. Gilles. Total iron is given as FeO.

I: Mn-rich childrenite from the arrojadite-aluminiferous alluaudite association.

II: coloured eosphorite from the heterosite-Na- and Mn-rich alluaudite association.

IIIa: colourless eosphorite from the lithiophilite-hureaulite association (Coll. Appl. Geol. 1371).

IIIb: coloured eosphorite from the same but altered association (Coll. Appl. Geol. 1370).

DESCRIPTION OF THE ASSOCIATIONS

Association I with arrojadite-alluaudite. In the beryl-muscovite-albite zone arrojadite, rimmed by alluaudite macroscopically, passes into albite, graphic structures previously recorded for the high aluminium content of alluaudite (Table II) (Fransolet, 1977). In this association eosphorite-childrenite aggregates, only detected under the polarizing microscope, corrode the albite crystals. These aggregates, with an irregular shape and a grain size of 0.5 mm maximum, are generally colourless. A few crystals are invaded by a yellow straw tint and show a distinct pleochroism. The use of X-ray diffraction presents problems, but the optical properties of the colourless grains (i.e. biaxial and negative, $2V_\alpha$ near 45°, a sharp dispersion $r < v$, and a birefringence in the region of 0.025) and the molecular proportions deduced from the analysis (Table I) corroborate the identification of an eosphorite-series member.

Practically constant in the same crystal, the ratio Fe/Mn fluctuates from one grain to another. The FeO contents vary between 15.40 and 18.20% and the MnO contents between 14.90 and 12.50%. These variations cannot be correlated with the pleochroism. Without a clear distribution law an average of the chemical data (Table I, column 1) yields an idealized composition $(Fe_{0.55}Mn_{0.45})AlPO_4(OH)_2 \cdot H_2O$ with $Fe/(Fe+Mn) = 0.548$, near the composition of Hagendorf 'childroeosphorite' (Strunz and Fisher, 1957).

Association II with heterosite-alluaudite. At the western contact of the pegmatite quartz core an important ferrisicklerite-heterosite mass shows well-developed alluaudite of bronze colour in frequent connection with white xenoliths reaching a size of 1 or 2 cm. Among these xenoliths, quartz with or without muscovite assemblages on one hand, and quartz-montebrasite (more or less replaced by white pinkish variscite) assemblages on the other, are observed. The second type affords ochre or orange-coloured fan- or rosette-like laths with a size of 2 or 3 mm. By X-ray diffraction this mineral appears to be a member of the eosphorite-childrenite series (Table III).

TABLE II. *Chemical compositions of the major associated phosphates*

	Association I		Association II		Association III
	Arrojadite*	Alluaudite*	Ferrisicklerite†	Alluaudite†	Lithiophilite†
P_2O_5	40.52	44.66	42.21	42.80	44.33
Al_2O_3	2.17	4.68	—	0.50	—
Fe_2O_3	—	—	28.22	28.42	0.00
FeO	25.72	23.91	1.33	0.98	14.94
MnO	18.63	19.66	20.20	18.61	30.74
MgO	0.21	0.46	0.61	0.59	0.06
CaO	2.03	0.36	0.60	0.67	0.10
Na_2O	6.27	7.10	0.08	4.33	0.04
K_2O	2.49	—	0.17	tr.	—
Li_2O	—	—	2.78	0.00	9.00
H_2O+	—	—	3.24	2.70	0.14
Insol.	—	—	0.60	0.19	0.63
Total	98.04	100.83	100.04	99.79	99.98
Cation proportions ($\times 10^3$)					
Al^{3+}	43	92	—	10	—
Fe^{3+}	—	—	353	356	—
Fe^{2+}	358	333	19	14	208
Mn^{2+}	263	277	285	262	433
$Fe_t/(Fe_t+Mn)$	0.576	0.546	0.566	0.585	0.324

* Chemical analyses performed by the Camebax electron microprobe (BRGM-CNRS). Analyst: C. Gilles. Total iron is given as FeO.

† Wet chemical analyses by J.-M. Speetjens.

The average of the chemical analyses (Table I, column 2) corresponds to a Fe-rich eosphorite composition near those from Newry or Rumford (Hurlbut, 1950), i.e. $(Mn_{0.66}Fe_{0.34})AlPO_4(OH)_2 \cdot H_2O$ with significative fluctuation of the Fe/(Fe+Mn) ratio.

The structural relationships between the different phases in the montebrasite xenoliths are rather obscure. Quartz, with a hypidiomorphic or xenomorphic shape, is riddled with undetermined opaque inclusions or prominently limpid. Montebrasite forms a fine-grained mosaic structure or well-developed crystals with cleavage and typical twins. Feathery eosphorite and montebrasite always present clear contacts. The latter phase is invaded by fine-grained puff-like aggregates of variscite, which also occurs with a spherolitic structure in the small fissures cross-cutting the whole association.

All the eosphorite crystals are definitely pleochroic with very intense yellow or brown absorption colours. Fig. 1*a* shows the rare case of a colourless eosphorite core preserved in a large coloured crystal. As it appears in fig. 1*b*, residual eosphorite is biaxial and negative with $2V_\alpha$ near 30° and the pleochroic mineral is biaxial and positive. The optical measurements on the latter give, for λ_{Na}, $\gamma = 1.710(4)$, $\beta = 1.694(4)$, and $\alpha = 1.690(4)$. $2V_\gamma$ varies from one grain to another, between 30 and 50°. The $r < v$ dispersion is very strong and the pleochroism very intense: γ = pale to gold yellow, β = slightly brownish yellow, and α = ochre to orange yellow. The refractive indices are clearly higher than these calculated by the relationships of Hurlbut (1950) or of Winchell (1958) for a Fe/(Fe+Mn) ratio = 0.341. Using the Gladstone and Dale rule, the molecular refractivities recently cheeked by Mandarino (1976) and taking a density 3.15 a little higher than the value fixed by the equation of Winchell (1958), the measured indices on the pleochroic eosphorite tend to demonstrate that an important amount of iron is ferric. The comparison with oxychildrenite is discussed below.

Association III with lithiophilite-hureaulite. At first weakly oxidized to sicklerite and then progressively replaced by colourless hureaulite (Fransolet, 1976), the lithiophilite masses frequently contain white xenoliths with amoeboidal borders and with a size smaller than 2 cm.

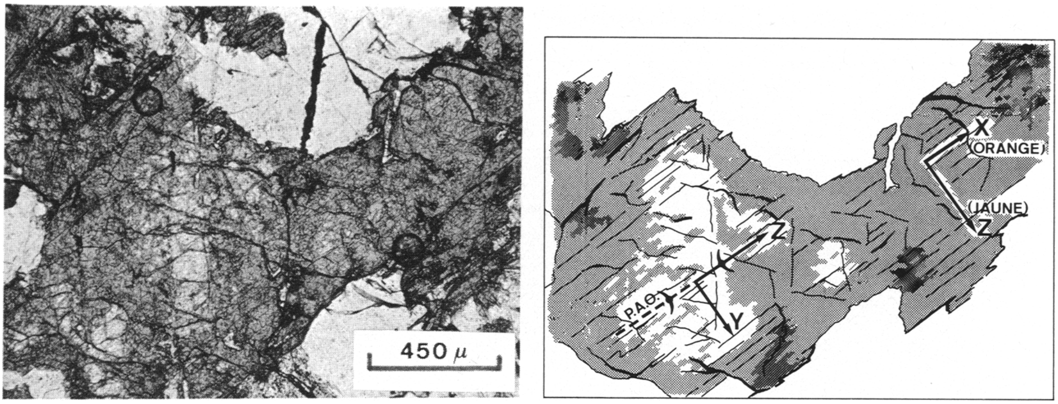

FIG. 1. *a*, left: Association II. Large monomineralic crystal of pleochroic eosphorite, orange-brown coloured and showing residual colourless eosphorite (left side of the picture). The other phase is quartz. Polarized light. *b*, right: Drawing of the same crystal indicating the optical orientations in the colourless part and in the strongly pleochroic zone.

In fresh lithiophilite (specimen 1371, Coll. Appl. Geol., Univ. Liège) residual microcline is full of eosphorite laths with a pink colour and a slightly pearly lustre, reaching 1 cm long. Under the microscope the xenoliths are constituted by large microcline crystals, practically unaltered and cross-cut by hypidiomorphic eosphorite. The finely crenelated borders of the latter clearly prove that it replaces feldspars. A few twinned montebrasite grains are also present in this association. At the contact of lithiophilite with microcline a thin and irregular rim (150 μm) of interstitial xenomorphic quartz (fig. 2) systematically occurs.

The fresh eosphorite, the powder pattern of which is similar to that of the Nahora material with a composition $(Mn_{0.76}Fe_{0.24})AlPO_4(OH)_2 \cdot H_2O$ (Correia Neves and Lopes Nunes, 1968) (Table III), seems to be particularly suitable to check the relationships of Hurlbut (1950) and Winchell (1958). With regard to the irregular cleavage, parallel to the absolutely colourless laths, the extinction is straight and the elongation positive. The $r < v$ dispersion is distinct. The measurements of $2V_\alpha$ give 47(2)°. For λ_{Na}, $\gamma = 1.663(1)$, $\beta = 1.658(1)$, and $\alpha = 1.637(1)$ with $2V_\alpha$ calculated = 51° 25′. The mineral compares fairly well

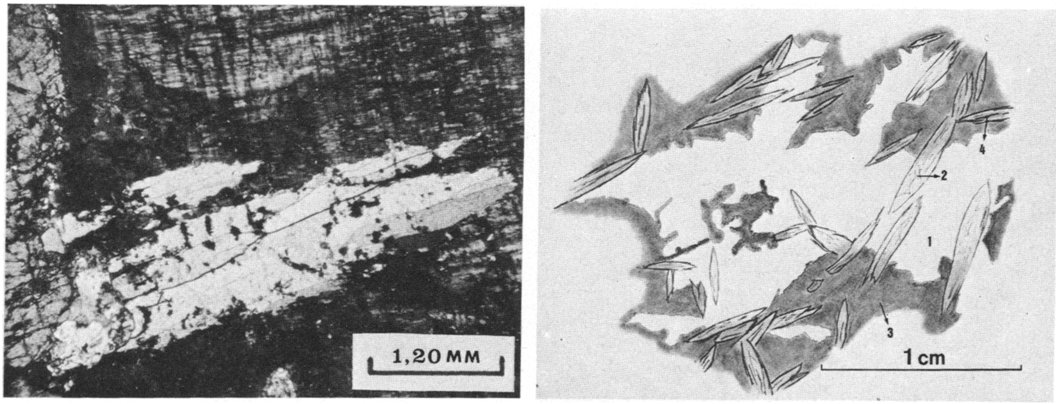

FIGS. 2 and 3: FIG. 2 (left). Association III. Colourless eosphorite (white) corroding microcline. On the left side of the picture lithiophilite (grey) is visible. Crossed polars. FIG. 3 (right). Association III. Drawing of a pinkish-white mass of quartz and variscite (1), which displays weakly tinged eosphorite crystals, (2) and which is progressively replaced by a quartz-cryptomelane mixture (3). In contact with Mn and Fe oxide minerals eosphorite is orange-yellow coloured (4).

TABLE III. *Eosphorite-childrenite series. X-ray powder patterns*

Buranga III		Nahora		Buranga II		Kalbinsky	
I/I_0	d (Å)	I/I_0	d (Å)	I/I_0	d (Å)	I/I_0	d (Å)
5	6.75	6	6.729	5	6.61		
						f	5.764
		3	5.306				
5	5.22	14	5.218	6	5.27	f	5.204
		1	5.005				
2	4.87	3	4.859				
5	4.38	10	4.382	6	4.37	m	4.295
4	4.12	8	4.125	6	4.10		
						m	4.022
4	3.54	9	3.542	5	3.508		
		1	3.467			m	3.484
4	3.40	6	3.404	3	3.376		
				2	3.299	m	3.305
		1	3.168				
2	3.07	2	3.081	2	3.094	f	3.095
		1	3.031	1	3.038		
1	2.91	2	2.904				
10	2.81	25	2.822	10	2.838	tF	2.825
				1	2.794		
2	2.61	3	2.608	2	2.623	f	2.630
		1	2.557	1	2.549	f	2.530
4	2.427	8	2.428	4	2.431	m	2.418
4	2.394	6	2.392	5	2.354	F	2.339
2	2.247	2	2.244	1	2.258	tf	2.261
		2	2.238				
1	2.191	1	2.188	1	2.194	m	2.181
1	2.132	2	2.138	1	2.144		
3	2.079	3	2.086	4	2.095	m	2.095
3	2.061	5	2.061	4	2.052	m	2.045
				1	2.023		
3	1.989	3	1.997	4	1.995	m	1.993
				1	1.953	f	1.944
2	1.914	2	1.917	2	1.924	f	1.918
2	1.872	4	1.873	4	1.869	m	1.865
1	1.805	1	1.804				
2	1,771	2	1.772	2	1.770	f	1.769
3	1.726	2	1.733	5	1,748	m	1.744
2	1.699	1	1.702				
2	1.680	2	1.685	1	1.687	tf	1.676
		1	1.673				
		1	1.636			tf	1.648
		1	1.621				
		1	1.601	1	1.612	tf	1.609
				2	1.558		
3	1.538	2	1.543	2	1.546	m	1.542
8	1.525	7	1.528	8	1.518	tF	1.514

Buranga III: colourless eosphorite from the association III (Debye-Scherrer camera, diam. 114.59 mm and Mn-filtered iron radiation).
Nahora: greenish eosphorite after Correia Neves and Lopes Nunes (1968) (diffractogram and FeKα radiation).
Buranga II: coloured eosphorite from the association II (conditions: see Buranga III).
Kalbinsky: oxychildrenite after Ginzburg and Voronkova (1950).

optically with Hebron, Poland, and Branchville eosphorite (Hurlbut, 1950). Winchell's equations yield a $Fe/(Fe+Mn)$ ratio $= 0.21 \pm 0.04$.

For different crystals the Fe/Mn ratio weakly fluctuates. The chemical composition (Table I, column 3) corresponds to $(Mn_{0.80}Fe_{0.20})AlPO_4(OH)_2 \cdot H_2O$ with a $Fe/(Fe+Mn)$ ratio in very good agreement with the results deduced from the optical properties.

In the more altered lithiophilite assemblages (specimen 1370, Coll. Appl. Geol., Univ. Liège) the presence of variscite, cryptomelane, quartz, and eosphorite in the xenoliths is detected by X-ray diffraction and under the microscope. Montebrasite is completely replaced by variscite. The powder diffractogram of the mixture shows weak intensity peaks assignable to montebrasite but the optical investigation cannot prove this observation. White to pinkish residual variscite and faintly coloured eosphorite laths have diffused borders and are progressively replaced by a quartz-cryptomelane mixture. This intense alteration of the xenoliths influences the eosphorite evolution. The eosphorite crystals isolated in the dark-grey oxides mass are indeed ochre- or orange-coloured. Some of them display a pale-yellow part bordered by variscite, and a brown or orange one in cryptomelane (fig. 3). This colour distribution in the eosphorite crystals finds itself once again for pleochroism in the thin sections. The intergranular joins and the fissures are filled up with cryptomelane screening the relationships between eosphorite and the other phases.

The variations of Fe/Mn ratio in the coloured crystals are again very slight. The average of the chemical data (Table I, column 4) corresponds, with a $Fe/(Fe+Mn)$ ratio $= 0.195$, to a composition pretty identical to the one that characterizes eosphorite in the fresh xenoliths.

Although this ratio is constant in the colourless and in the pleochroic crystals, noticeable differences appear in the refractive indices. The measurements on the pleochroic mineral give for λ_{Na}: $\gamma = 1.695(2)$, $\beta = 1.689(2)$, and $\alpha = 1.670(2)$. Eosphorite is still biaxial and negative with $2V_\alpha$ varying between 30 and 45°. The $r < v$ dispersion is strong and the very intense pleochroism is γ = very pale yellow, β and α = orange yellow. By analogy with the case of association II the high values for the refractive indices could be accounted for by the presence of a large content of ferric iron.

DISCUSSION

Before considering the geochemical features and the formation processes the observations show that a determination problem must be approached:

Identification of $(Mn,Fe)AlPO_4(OH)_2 \cdot H_2O$ *phases*

Although the eosphorite-childrenite series minerals are generally quoted as colourless phases, the investigation of grains and thin sections reveals frequent and intensively pleochroic terms occurring in the Buranga mine. In each association these phosphate minerals systematically afford an alteration process that invades the colourless crystals from their borders and through the cleavages and fissures, and progressively colours them pale yellow and afterwards orange-brown. This property constitutes a distinctive character for certain minerals, rather similar to the eosphorite series members but richer in Fe^{3+} [and even in Mn^{3+}], such as ernstite $(Mn,Fe^{3+})AlPO_4(OH,O)$ (Seeliger and Mücke, 1970) and oxychildrenite $(Mn^{2+},[Mn^{3+},]Fe^{3+})AlPO_4(O,OH) \cdot 1.5H_2O$ (Ginsburg and Voronkova, 1950).

The powder patterns of orange-coloured eosphorite (association II) and colourless (association III) are set out in Table III. The powder pattern of the coloured eosphorite (association III) is not given because it is definitely identical to that one obtained for the colourless mineral from the same association. By the absence of the intense doublet at 2.836-2.829 Å, typical for ernstite, this mineral species has not been identified in Buranga. The powder pattern of the coloured phase (column 3) shows a distinctive shifting of a few rather intense peaks. Owing to the lack of accurate data about the crystallographic properties in relationship with the chemical composition of the eosphorite-childrenite series, these shiftings presently remain without explanation. So the identification of oxychildrenite by this means is not much reliable. Without the water determination and the chemical distinction of ferrous and ferric iron only the optical properties can be considered.

In this domain the results clearly diverge from the commonly known data for the eosphorite-childrenite series. Moreover, they cannot be employed to certify the presence of oxychildrenite in Buranga. Indeed the knowledge of the optical sign of this mineral is completely confused. After Ginzburg and Voronkova (1950) oxychildrenite is biaxial and negative; however, using their measured refractive indices, the calculation gives $2V_\gamma = 52° 32'$. Mirtshing (1950) indicates a negative sign and Fleischer (1951) records a positive one. Finally the pleochroism described by the Russian authors is the opposite to that observed in Buranga.

Since the refractive indices of the pleochroic material from Buranga cannot be correlated with the $Fe^{2+}/(Fe^{2+}+Mn)$ ratio obtained from the chemical analyses (Table I), a notable amount of ferric iron in these minerals is probable; in this case, and considering the similarities between the powder patterns, these phosphate minerals can only be called oxidized eosphorites and childrenites.

The geochemical features

The oxidation process in the eosphorite-childrenite series. This oxidation phenomenon is particularly well developed in association II (fig. 1*a* and *b*) and in the fig. 3 where eosphorite is more coloured near cryptomelane. The investigation of the colourless and pleochroic terms by electron microprobe shows that the modifications of the optical properties are not due simply to a variation of the Fe/Mn ratio.

These modifications, described in the preceding paragraphs and probably induced by the presence of ferric iron, resemble those observed in the transformation of phosphoferrite into landesite-kryzhanovskite in Mangualde (Fransolet, 1975). After Moore and Araki (1976) this transformation forms a continuous series between $Fe_3^{2+}(H_2O)_3(PO_4)_2$ and $Fe_3^{3+}(OH)_3(PO_4)_2$, thanks to an auto-oxidation reaction $2Fe^{2+}(H_2O) \rightarrow 2Fe^{3+}(OH)^- + H_2\nearrow$.

Since Hanson (1960) has reported, in the atomic structure of eosphorite $(Mn,Fe)O_4(OH)_2$ and $AlO_2(OH)_2(H_2O)_2$ octahedra chains indicating a particular structural role for the water molecules, that type of reaction is not justified in the present case. When the oxidation reaction $2Fe^{2+}(OH)_2^- \rightarrow 2Fe^{3+}O^{2-} + H_2\nearrow$ is considered, such as it occurs in oxidized rockbridgeite without a modification of the atomic arrangement (Moore, 1970), a similar process may be suggested in the eosphorite structure too, leading to the existence of a continuous isomorphic series between $(Mn_{1-x}Fe_x^{2+})AlPO_4(OH)_2 \cdot H_2O$ and $(Mn_{1-x}Fe_x^{3+})AlPO_4(OH)_{2-x}O_x \cdot H_2O$ with intermediate terms containing both Fe^{2+} and Fe^{3+}. This progressive oxidation would involve an absorption phenomenon, first in the yellow tinges and afterwards in the orange-brown colours, as the Fe^{3+} content increases.

The Fe/Mn ratio. Although the electron microprobe did not reveal $Fe_t/(Fe_t+Mn)$ variations during the oxidation processes, the point analyses made on different crystals from the same association show weak fluctuations of this ratio. In the chemical data used by Hurlbut (1950) such variations were observed from an extremity to the other of well-developed crystals.

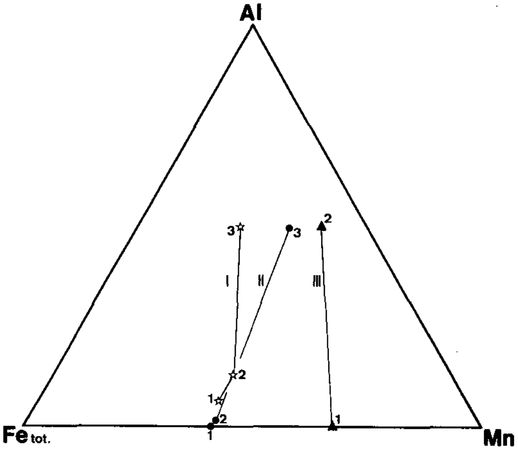

FIG. 4. Ternary Al-Fe-Mn diagram showing the composition of the eosphorites *s.l.* (Table I) and of the major associated phosphates (Table II). Association I: 1 = arrojadite; 2 = aluminiferous alluaudite; 3 = Mn-rich childrenite. Association II: 1 = ferrisicklerite; 2 = Na- and Mn-rich alluaudite; 3 = eosphorite. Association III: 1 = lithiophilite; 2 = eosphorite.

In the three described associations each (Mn,Fe) $AlPO_4(OH)_2 \cdot H_2O$ term is characterized by a mean $Fe_t/(Fe_t + Mn)$ ratio, which is different but in prominent relationship with the same ratio in the other essential phosphates of these assemblages (Table II). It clearly appears in the Al-Fe-Mn ternary diagram (fig. 4) where total iron is considered and where the compositions are plotted following the cations numbers deduced from the chemical analyses (Table II). The Fe_t/Mn ratio of the initially formed phases (arrojadite, Li(Fe,Mn) PO_4 series) tends to move to the Mn pole. A similar shifting of this ratio is observed for the associated eosphorite-childrenite group members, as if the Fe and Mn contents of the latter were ruled by the Fe_t/Mn ratio of the mother phases. Moreover, $Fe_t/(Fe_t + Mn)$ is not preserved during the eosphorite *s.l.* deposition and is lower in it than in the anteriorly crystallized phosphate minerals. As these observations presently concern only three associations from the Buranga pegmatite, this conspicuous dependence of the Fe/Mn ratio and its behaviour in the eosphorite-childrenite series need further investigation.

The genetic process

In the present state of the investigations the discussion about the genetic process of the eosphorite-childrenite series minerals must be restricted to the case of the Fe- and Mn-rich phosphates assemblages from the Buranga mine only. Moreover, it concerns three associations rather different in their mineral content. Nevertheless, new observations, on one hand, and a few assumptions, on the other hand, might throw some additional light on the deposition mechanism of $(Mn,Fe)AlPO_4(OH)_2 \cdot H_2O$ minerals associated with phosphates, frequently recorded in the granitic pegmatites.

Replacement of feldspars. The investigation of the structural relationships in the associations I and III obviously shows the replacement of albite by childrenite and of microcline by eosphorite associated with montebrasite. The destabilization of rather fresh Na- or K-feldspars yields aluminium indispensable to the growth of these phosphates. The general aspect of the associations and the texture of these minerals suggest a typical phenomenon of hydrothermal alteration. That seems to depict again the instability of Al-silicates in contact with solutions rich in phosphates probably as H_3PO_4 and can connect the conclusions of Wise and Loh (1976).

Relationships between eosphorite and montebrasite. In two of the three described associations eosphorite coexists with montebrasite more or less transformed into variscite. Generally in Buranga the $LiAlPO_4(OH,F)$ series members are not altered by eosphorite *s.l.*; in the present case the intergranular joins between these two phosphates are absolutely clear. Such a close association is already known in the Patrimonio pegmatite, Paraiba, Brasil (Murdoch, 1955), and in the Nahora mine, Alto Ligonha, Mozambique (Correia Neves and Lopes Nunes, 1968). The association of montebrasite and eosphorite *s.l.* could constitute a genuine paragenesis. So, microcline xenoliths isolated in fresh lithiophilite (association III) are simultaneously corroded by montebrasite and eosphorite. In association I where albite is replaced by childrenite only, the absence of montebrasite could be due to absence or scarcity of lithium in arrojadite and in Al-bearing alluaudite. These facts could be tentatively considered as a new argument showing the dependence of the montebrasite-eosphorite paragenesis on the chemical composition of the formerly developed phosphates. In other words, the Fe/Mn ratio of the $(Mn,Fe)AlPO_4(OH)_2 \cdot H_2O$ phase and the deposition of associated montebrasite would be directly connected to the chemical nature of the hydrothermal solutions in close contact with the 'primary' phosphate minerals and likely to corrode directly adjacent feldspars.

Eosphorite deposition and evolution of the Li-Fe-Mn-rich phosphate minerals. A definite knowledge of the period of feldspar alteration by hydrothermal fluids giving eosphorite *s.l.* and, contingently, montebrasite is not yet possible.

However, in the evolutive mechanism of the Li-Fe-Mn phosphate assemblages, a relatively early process may be assumed.

If the existence of a eosphorite-montebrasite paragenesis depending on the chemical composition of the formerly crystallized phosphates is considered, the occurrence of $LiAlPO_4(OH,F)$ in the association II with a $Li(Fe,Mn)PO_2$ member completely oxidized would infer that the deposition of eosphorite and montebrasite takes place into the silicate xenoliths before the stage of Li-leaching and oxidation giving ferrisicklerite and heterosite. This leaching stage might be likely to supply the montebrasite formation with Li although the physical and chemical conditions for Li-leaching and $Li(Fe,Mn)PO_4$ oxidation are not known presently. Such an assumption is not justified in the association III in which the fresh lithiophilite crystals do not display any oxidation phenomenon (i.e. sicklerite occurrence) at the contact of microcline corroded by eosphorite and montebrasite.

The arguments are presently lacking to specify the relationships between the $(Mn,Fe)AlPO_4(OH)_2H_2O$ minerals deposition and the Na-Mn-rich alluaudites, because the formation of the latter would be anterior to the formation stage of the ferrisicklerite and heterosite phases (Fransolet, 1977).

Oxidation of the eosphorite-childrenite series. As it is described here, the oxidation of the eosphorite-childrenite series seems to be a late process, taking in account the observations made on the three associations from the Buranga pegmatite.

In the association II, the cleavages of alluaudite, heterosite, and the xenolith minerals, their intergranular joins and numerous veinlets are filled by Mn oxide products. The altered masses of the association III (fig. 3) clearly show intensively coloured eosphorite crystals in close contact with cryptomelane. These facts tend to suggest that the eosphorite oxidation and the cryptomelane deposition are two contemporaneous phenomena.

Conclusions

Thanks to a chemical investigation by electron microprobe complemented by X-ray diffraction and by optical measurements, an autoxidation process of the eosphorite-childrenite group members is suggested. During this phenomenon, contemporaneous with the replacement of phosphates by Mn oxides, the ratio of the transition metal cations is preserved. A reinvestigation of the mineralogical properties of oxychildrenite is necessary and an atomic-structure analysis must specify the autoxidation process in the pleochroic members.

From the structural relationships the existence of a montebrasite-eosphorite paragenesis is assumed. It takes place during the hydrothermal alteration of Na- or K-feldspars in close association with Li-Fe-Mn-rich phosphates. The chemical properties of the hydrothermal fluids are locally influenced by the chemical composition of the earlier formed phosphates. This relationship might suggest that eosphorite *s.l.*, possibly associated with montebrasite, would have formed before the oxidation stage, i.e. the ferrisicklerite-heterosite development. So, in the Fe- and Mn-rich phosphates assemblages from the Buranga pegmatite, the eosphorite-childrenite series members constitute evidence for a reaction of the alumino-silicates in presence of phosphorus-bearing hydrothermal fluids and this alteration would be relatively early in the evolutive mechanism of the $Li(Fe,Mn)PO_4$ minerals.

Acknowledgements. The present work was carried out at the Institut für Mineralogie, Ruhr-Universität Bochum, during the tenure of a fellowship (1978-9) awarded by the Alexander von Humboldt Foundation, FRG. Sincere thanks are extended for financial help by the Foundation. The author is thankful to MM R. Pierrot, J. Halfon, G. Remond, and C. Gilles for the analyses performed by the BRGM-CNRS electron microprobe. Thanks are due to the National Foundation for Scientific Research of Belgium, which financially supported the trip to Rwanda, and to the Géomines and Somirwa Societies, which kindly helped the field-work in the Gatumba area. Additional samples from Buranga were kindly provided by Professor P. Evrard (University of Liège). The manuscript was critically reviewed by Dr F. Permingeat and Dr M. Hey who corrected it for language also.

REFERENCES

Correia Neves (J. M.) and Lopes Nunes (J. E.), 1968. *Rev. Ciênc. Geol.*, Lourenço Marques, **1**, ser. A, 1-48.

Fleischer (M.), 1951. *Am. Mineral.* **36**, 642.

Fransolet (A.-M.), 1975. Étude minéralogique et pétrologique des phosphates des pegmatites granitiques. Thèse de doctorat. Inst. Minéralogie, Université de Liège (unpublished).

—— 1976. *Bull. Soc. fr. Minéral. Cristallogr.* **99**, 261-73.

—— 1977. Ibid. **100**, 348-52.

Ginzburg (A. I.) and Voronkova (N. V.), 1950. *Dokl. Acad. Nauk. SSSR*, **71**, 145-8. (In Russian.)

Hanson (A. W.), 1960. *Acta Crystallogr.* **13**, 384-7.

Hurlbut (C. S., *Jr.*), 1950. *Am. Mineral.* **35**, 793-805.

Mandarino (J. A.), 1976. *Can. Mineral.* **14**, 498-502.

Mirtsching (A.), 1950. *Zentralbl. Mineral.* **1**, 162-3.

Moore (P. B.), 1970. *Am. Mineral.* **55**, 135-69.

—— and Araki (T.), 1976. *Inorg. Chem.* **15**, 316-21.

Murdoch (J.), 1955. *Am. Mineral.* **40**, 50-63.

Remond (G.), Giraud (R.), Conty (C.), and Tong (M.), 1977. *Proc. 8th internat. Conf. on X-ray optics and microanalysis*, 18-24 August 1977, Boston, Mass., U.S.A., no. 186.

Seeliger (E.) and Mücke (A.), 1970. *Neues Jahrb. Mineral. Mh.* **1970,** 289-98.

Strunz (H.) and Fisher (M.), 1957. Ibid. **1957,** 78-88.

Von Knorring (O.), 1965. *Bull. Serv. Géol. Républ. Rwanda,* **2,** 11-14.

—— 1970. Mineralogical and geochemical aspects of pegmatites from orogenic belts of equatorial and southern Africa, 157-84. *In* African Magmatism and Tectonics, ed. Clifford (T. N.) and Gass (I. G.), Oliver & Boyd, Edinburgh.

Winchell (H.), 1958. *Am. Mineral.* **43,** 765-8.

Wise (W. S.) and Loh (S. E.), 1976. Ibid. **61,** 409-13.

[*Manuscript received 16 November 1979;*
revised 7 February 1980]